International Journal of Solids and Structures 129 (2017) 146–155

Contents lists available at ScienceDirect

International Journal of Solids and Structures

journal homepage: www.elsevier.com/locate/ijsolstr

An analysis of edge dislocation pileups against a circular inhomogeneity or a bimetallic interface

Vlado A. Lubarda[1]

Department of NanoEngineering, University of California, La Jolla, San Diego, CA 92093-0448, USA

ARTICLE INFO

Article history:
Received 6 May 2017
Revised 31 August 2017
Available online 5 September 2017

Keywords:
Bimetallic interface
Configurational force
Dislocation pileup
Edge dislocation
Inhomogeneity
Stress concentration

ABSTRACT

Equilibrium configurations of edge dislocation pileups against a circular inhomogeneity or a bimetallic interface are determined numerically for a given number N of dislocations, the applied shear stress τ, the size of the inhomogeneity, and the degree of material disparity. The increase of applied stress moves a pileup closer to the inhomogeneity and increases the density of dislocations within a pileup, which is more pronounced for smaller and softer inhomogeneities due to their weaker repulsion of dislocations. The configurational force exerted by the pileup on a circular inhomogeneity is equal to $N\tau b_x$, where b_x is a Burgers vector of dislocations, plus a term dependent on dislocation positions and material properties. The configurational force on a bimetallic plane interface is equal to $N\tau b_x$, independently of dislocation positions and material properties. The stress concentration caused by dislocation pileups against different interfaces is evaluated and discussed, which is of importance for the study of interface cracking. In general, the increase of the shear modulus and the Poisson ratio disparities (G_2/G_1 and ν_2/ν_1, where the subscript 1 specifies the material in which dislocations reside) diminishes the interface stresses.

1. Introduction

An analysis of stress field caused by dislocation pileups against material inhomogeneities such as second-phase particles and grain boundaries is of importance for the study of various features of inelastic material response. For example, the grain-size dependence of a polycrystalline yield strength and the corresponding Hall–Petch relation can be explained by the build-up of stresses caused by a dislocation pileup against the grain boundary and the activation of the Frank–Reed dislocation sources in a neighboring grain. The onset of the Stroh–Zener interface crack, or the crack ahead of the Lomer–Cottrell lock at the intersection of two slip planes, can be explained by the build-up of a tensile stress below the leading dislocation of the pileup, or in front of the locked-in dislocation. An early study of edge and screw dislocation pileups in an infinite homogeneous medium was performed by Eshelby et al. (1951), who assumed that the leading dislocation in the pileup was pinned (locked) in its position by an imposed force which prevented its glide. Chou (1965) considered a screw dislocation pileup against a rigid boundary of a semi-infinite elastic medium. Barnett and Tetelman (1966); 1967),Thölén (1970), and Smith (1972) solved the problem of a screw dislocation pileup against a circular inhomogeneity. The methods based on either discrete or continuously distributed dislocations were used in these analyzes. Barnett (1967) derived an exact solution for the distribution of a pileup of screw dislocations near a bimetallic interface formed by welding together two elastic half-planes of different shear moduli. Chou (1966) considered discrete edge dislocation pileups against a bimetallic interface and examined numerically the relationship between the length of the pileup, number of dislocations, and the applied stress, for given material properties. Based on the method of continuously distributed dislocations, Kuang and Mura (1968) solved analytically the singular integral equations for the equilibrium positions of both edge and screw dislocation pileups against a bimetallic interface. The integral equation for edge dislocations was solved by a Wiener–Hopf method with Mellin transforms, but the solution involves infinite products, whose evaluation is numerically quite demanding. Discrete edge dislocation pileups against a bimetallic interface were investigated numerically by Kuan and Hirth (1976), who included in their analysis nonlinear dislocation core terms. They examined the implication of their results with respect to stress concentrations at the interface and the tendency for fracture or flow initiation. Wagoner (1981) studied dislocation pileups against planar grain boundaries employing full anisotropic elastic solutions, single-crystal anisotropic approximations, and isotropic approximations. Öveçoğlu et al. (1987) considered discrete edge dislocation pileups against a bimetallic interface and examined the effects of applied stress, pileup length, and

E-mail address: vlubarda@ucsd.edu

[1] Dedicated to Professor David M. Barnett for his inspiring contributions to dislocation mechanics.

http://dx.doi.org/10.1016/j.ijsolstr.2017.09.004
0020-7683/

the elastic properties of the two phases on the distribution of dislocations in the pileup and on the stresses at the interface. More recent work includes contributions by Voskoboinikov et al. (2007; 2009), and Hall (2010).

A study of edge dislocation pileups against a cylindrical circular inhomogeneity was not previously reported in the literature, to the best of our knowledge, and we thus consider such pileups in Section 2 of this paper. The pileups are formed by a remotely applied uniform shear stress. The equilibrium positions of dislocations are determined by solving numerically the system of N nonlinear algebraic equations representing the equilibrium conditions of the vanishing Peach–Koehler force for each dislocation in the pileup. The method of continuous distribution of edge dislocations is not used because of the difficulties in solving the corresponding singular integral equations, although large radius inhomogeneities could possibly be handled by a perturbation analysis of the half-space continuous distribution solution (as pointed out to me by one of the reviewers). Furthermore, for small micron-size grains in a polycrystalline sample at the onset of plastic yield, when the dislocation density is of the order of $10^8/\text{cm}^2$ or so, only dozens of dislocations may participate in a pileup at the grain boundary, so that their discrete dislocation model may be more adequate. The image-type contribution to the Peach–Koehler force from the interaction of the dislocation with the inhomogeneity is calculated by using the stress field around an edge dislocation near a circular inhomogeneity, derived by Dundurs and Mura (1964). The contribution to the dislocation force from a remotely applied shear stress is determined from the known stress field around the inhomogeneity in an infinite medium under a remote shear loading. The increase of the applied stress moves a pileup closer to the inhomogeneity and increases the density of dislocations within the pileup. This is more pronounced for a smaller and softer inhomogeneities, due to their weaker repulsion of dislocations. We derive the configurational force exerted on the inhomogeneity by a pileup, which is expressed in terms of the sum of the local Peach–Koehler forces from the remote loading only, and thus is equal to $N\tau b_x$ plus a term dependent on dislocation positions and material properties. The magnitude of the shear stress at the interface between the inhomogeneity and the medium along the slip plane of dislocations is also evaluated. This stress decreases with the increase of the ratio $\Gamma = G_2/G_1 > 1$ between the shear stiffness of the inhomogeneity and the surrounding matrix. In Section 3 we used the same approach as Öveçoğlu et al. (1987) to shed additional light on edge dislocation pileups against a plane bimetallic interface. If σ_x^τ due to applied shear stress τ has its maximum along the interface at $y = y_*$, $\sigma_x^{c\tau}$ due to the shear stress $c\tau$ has its maximum at $y = y_*/c$ and $(\sigma_x^{c\tau})_{\max} = c(\sigma_x^\tau)_{\max}$. Similar property holds for the shear stress along the interface, except that the maximum of σ_{xy} always occurs at the intersection of the slip plane and the interface. We also discuss the dependence of the magnitude of stress concentration at the interface on the shear moduli and Poisson's ratios of two materials, which is of importance for the study of interface cracking. In general, the increase of the shear modulus and Poisson's ratio disparities (G_2/G_1 and ν_2/ν_1) diminishes the interface stresses due to the stronger repulsion exerted by such interface on the piled-up dislocations.

2. Edge dislocation pileup against a circular inhomogeneity

Fig. 1a shows an edge dislocation with a Burgers vector b_x at a distance x_i from the center of a circular (cylindrical) inhomogeneity of radius a imbedded in an infinite elastic isotropic medium. The elastic properties of the medium are (G_1, ν_1), and of the inhomogeneity (G_2, ν_2). The shear stress along the x-axis, outside of the inhomogeneity, is specified by (Dundurs and Mura, 1964)

$$\hat{\sigma}_{xy}^{\text{disl}}(x,0) = \frac{2}{\xi-\xi_i} + (A+B)\frac{\xi_i}{\xi\xi_i - 1} + 2A\frac{(\xi-\xi_i)(\xi_i^2-1)}{(\xi\xi_i-1)^3} - \frac{A+B}{\xi} + \frac{A-B}{\xi^2\xi_i} + \frac{2A}{\xi^3}, \tag{1}$$

where

$$\xi = \frac{x}{a}, \quad \xi_i = \frac{x_i}{a}, \quad \hat{\sigma}_{xy} = \frac{\sigma_{xy}}{k_1(b_x/a)} \quad k_1 = \frac{G_1}{\pi(\kappa_1+1)}, \tag{2}$$

The utilized material parameters are

$$A = \frac{\Gamma-1}{1+\kappa_1\Gamma}, \quad B = \frac{\kappa_1\Gamma-\kappa_2}{\kappa_2+\Gamma}, \quad \Gamma = \frac{G_2}{G_1}, \tag{3}$$

with the Kolosov constants $\kappa_1 = 3-4\nu_1$ and $\kappa_2 = 3-4\nu_2$. It is noted that the constants A and B in (3) are opposite in sign to those used by Dundurs and Mura (1964). The stress is normalized by $k_1(b_x/a)$, so that the right-hand side of (1) is independent of the ratio a/b_x, which will be convenient for the subsequent presentation and interpretation of numerical results.

The non-singular part of the shear stress at $x = x_i$ is

$$\hat{\sigma}_{xy}^{\text{disl}}(x_i,0) = \frac{1}{\xi_i}\left(\frac{A+B}{\xi_i^2-1} + \frac{3A-B}{\xi_i^2}\right). \tag{4}$$

If the medium is subjected to a remotely applied stress $\sigma_{xy}^\infty = -\tau$, the shear stress along the x-axis, outside of the inhomogeneity, is (e.g., Lubarda and Markenscoff, 1999)

$$\hat{\sigma}_{xy}^{\text{appl}}(x,0) = -\hat{\tau}\left[1 - A\left(\frac{2}{\xi^2} - \frac{3}{\xi^4}\right)\right], \quad \hat{\tau} = \frac{\tau}{k_1(b_x/a)}. \tag{5}$$

The configurational force exerted by the inhomogeneity on the dislocation at $x = x_i$ is the image force from that dislocation with respect to the inhomogeneity, $f_{i,i}^{\text{image}} = \sigma_{xy}^{\text{disl}}(x_i,0)b_x$. In a dimensionless form, in view of (4), this is

$$\hat{f}_{i,i}^{\text{image}} = \hat{\sigma}_{xy}^{\text{disl}}(x_i,0) = \frac{1}{\xi_i}\left(\frac{A+B}{\xi_i^2-1} + \frac{3A-B}{\xi_i^2}\right), \quad \hat{f} = \frac{f}{k_1 b_x^2/a} \tag{6}$$

The configurational force exerted on the dislocation by the externally applied remote stress τ is, $f_i^{\text{appl}} = \sigma_{xy}^{\text{appl}}(x_i,0)b_x$, or, in view of (5),

$$\hat{f}_i^{\text{appl}} = \hat{\sigma}_{xy}^{\text{appl}}(x_i,0) = -\hat{\tau}\left[1 - A\left(\frac{2}{\xi_i^2} - \frac{3}{\xi_i^4}\right)\right]. \tag{7}$$

If there are two alike edge dislocations near a circular inhomogeneity, one at a distance $x = x_i$ and the other at a distance $x = x_j$ from the center of the inhomogeneity (Fig. 1b), there is an additional contribution to the force on the dislocation at $x = x_i$ due to its interaction with the dislocation at $x = x_j$. This is $f_{i,j} = f_{i,j}^\infty + f_{i,j}^{\text{image}}$, where $f_{i,j}^\infty$ is the interaction force between the two dislocations if they were in an infinite medium, while $f_{i,j}^{\text{image}}$ is the image part of the force due to the presence of the inhomogeneity. From expression (1), these are, in a dimensionless form,

$$\hat{f}_{i,j}^\infty = \frac{2}{\xi_i - \xi_j}, \tag{8}$$

$$\hat{f}_{i,j}^{\text{image}} = \frac{A+B}{\xi_i\xi_j - 1}\gamma_j + 2A\frac{(\xi_i-\xi_j)(\xi_j^2-1)}{(\xi_i\xi_j-1)^3} - \frac{A+B}{\xi_i} + \frac{A-B}{\xi_i^2\xi_j} + \frac{2A}{\xi_i^3}. \tag{9}$$

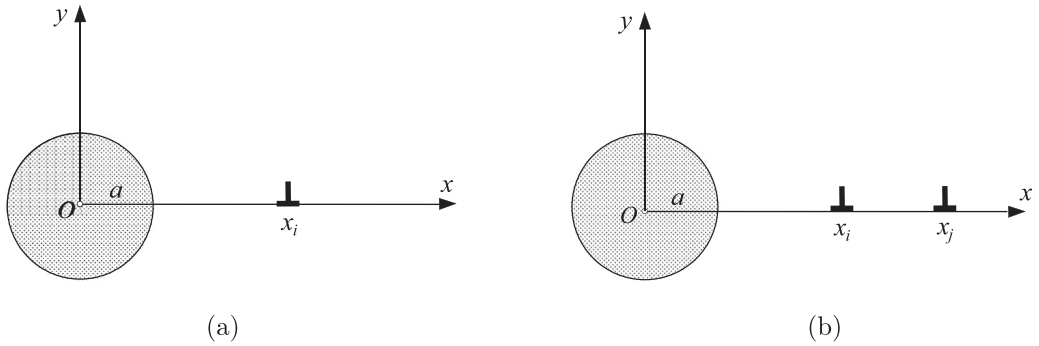

Fig. 1. (a) An edge dislocation at a distance x_i from the center of a circular inhomogeneity of radius a in an infinite medium. (b) Two edge dislocations near a circular inhomogeneity at the positions x_i and x_j.

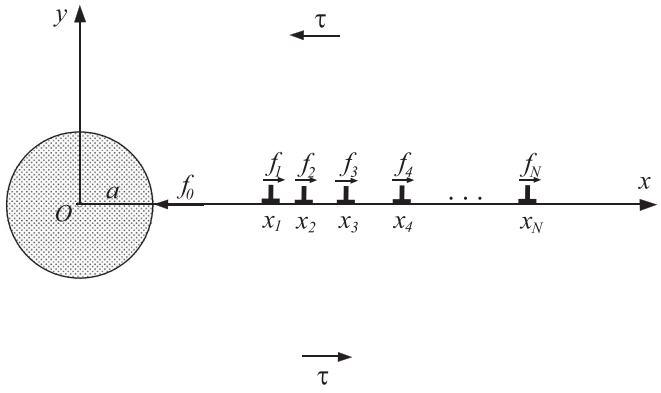

Fig. 2. A pileup of N edge dislocations against a circular inhomogeneity of radius a within an infinite medium. The applied remote uniform shear stress is τ. The configurational force exerted on the inhomogeneity by the pileup is f_0. In the equilibrium configuration the configurational force on each dislocation vanishes ($f_i = 0$), which specifies the corresponding positions of dislocations x_i ($i = 1, 2, 3, \ldots, N$).

2.1. Edge dislocation pileup

If there are N dislocations in a pileup of edge dislocations (Fig. 2), the total force on a dislocation at x_i is

$$f_i = f_i^{\text{appl}} + \sum_{j=1}^{N} f_{i,j}^{\text{image}} + \sum_{j\neq i}^{N} f_{i,j}^{\infty} . \tag{10}$$

In the pileup equilibrium configuration, the dislocation force on each dislocation vanishes ($f_i = 0$), which defines a system of N nonlinear algebraic equations for the equilibrium dislocation positions. Expressed in a dimensionless form, this is

$$\hat{f}_i^{\text{appl}} + \sum_{j=1}^{N} \hat{f}_{i,j}^{\text{image}} + \sum_{j\neq i}^{N} \hat{f}_{i,j}^{\infty} = 0 , \quad (i = 1, 2, 3, \ldots N) , \tag{11}$$

where $\hat{f}_i^{\text{appl}}$, $\hat{f}_{i,j}^{\text{image}}$, and $\hat{f}_{i,j}^{\infty}$ are specified by (7)–(9). For a given N, this system of nonlinear equations was solved numerically by using the *fsolve* function within the Matlab software. Among three available iterative algorithms, *fsolve* chooses by default the trust-region dogleg algorithm based on the interior-reflective Newton method and the method of preconditioned conjugate gradients (Coleman and Li, 1994; Conn et al., 2000). Details of the numerical procedure based on an interior penalty function method, in which numerical solution is sought by solving a sequence of unconstrained minimization problems, are given by Öveçoğlu et al. (1987). It is assumed that the applied stress is small enough to ensure that $(x_1 - a)$ and $(x_i - x_{i-1})$ are all sufficiently large compared with b_x to ensure that dislocation cores do not overlap. The solid line curves in Fig. 3 specify the equilibrium positions of dislocations for $N = 5$ and $N = 10$, corresponding to different levels of the applied shear stress τ (scaled by $k = k_1 b_x/a$). This scaling factor is used so that the curves shown in Figs. 3 and 4 apply for all finite ratios of a/b_x. The inhomogeneity was assumed to be rigid, so that $A = 1/\kappa_1$ and $B = \kappa_1$. The Poisson ratio was taken to be $\nu_1 = 1/3$. The increase of the applied stress moves the pileup closer to the inhomogeneity and increases the density of dislocations within the pileup. Fig. 4a shows the position of the leading dislocation x_1 in the pileup, and Fig. 4b the extent (length) of the pileup ($L = x_N - x_1$) vs. the applied shear stress τ, in the case $N = 5$. In view of the normalizing factors utilized, it follows that for larger inhomogeneities (larger ratio a/b_x), the repulsion from the inhomogeneity is stronger, thus larger are the ratios x_1/b_x and L/b_x, for any given level of applied shear stress τ. The repulsion is also stronger for stiffer inhomogeneities, as illustrated in Fig. 5. The Poisson ratios also have the effect: the increase of ν_2/ν_1 increases the repulsion exerted on dislocations by the inhomogeneity.

The dashed curves in Figs. 3 and 4 specify the equilibrium positions of the pileup dislocations in the absence of the inhomogeneity, obtained from the classical solution of Eshelby et al. (1951), who assumed that the leading dislocation in the pileup in an infinite medium is locked (see, also, Hirth and Lothe, 1982). In this case, if the locked dislocation is at $x_1 = 0$, the total force on a dislocation at $x_i (i > 1)$ is $f_i = -\tau b_x + \sum_{j\neq i} f_{i,j}^{\infty} + 2k_1 b_x^2/x_i$, where $f_{i,j}^{\infty} = 2k_1 b_x^2/(x_i - x_j)$. The total force required to hold the locked dislocation in equilibrium is $N\tau b_x$. The dislocations in such pileup are closer to the leading dislocation, because of the absence of the inhomogeneity and its repulsive effect on the pileup.

2.2. Configurational force on a circular inhomogeneity

Configurational forces between two material defects obey the law of action and reaction. Thus, the configurational force on a circular inhomogeneity from the dislocation at x_i in the pileup of N dislocations is the same in magnitude but opposite in direction to the configurational force on the dislocation at x_i from the image effects of all dislocations in the pileup with respect to the inhomogeneity, i.e.,

$$f_i^{\text{inhom}} = \sum_{j=1}^{N} f_{i,j}^{\text{image}} . \tag{12}$$

The total configurational force on the inhomogeneity, directed to the left, is

$$f_0 = \sum_{i=1}^{N} f_i^{\text{inhom}} = \sum_{i=1}^{N}\sum_{j=1}^{N} f_{i,j}^{\text{image}} . \tag{13}$$

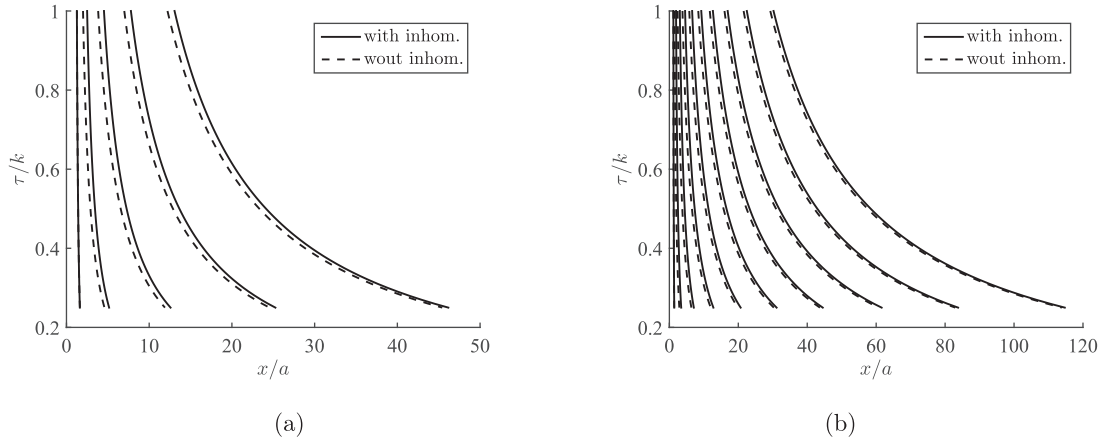

Fig. 3. (a) The equilibrium positions $\xi = x/a$ of $N = 5$ dislocations in a pileup against a rigid circular inhomogeneity of radius a vs. the applied shear stress τ (solid line curves). The Poisson ratio $\nu_1 = 1/3$. The dashed curves specify the equilibrium positions in the absence of the inhomogeneity, with the leading dislocation in the pileup being pinned. (b) The same as in (a) for $N = 10$. The utilized normalizing factor for τ is $k = k_1 b_x/a$, with k_1 specified by (2), so that the shown curves apply for any ratio of a/b_x.

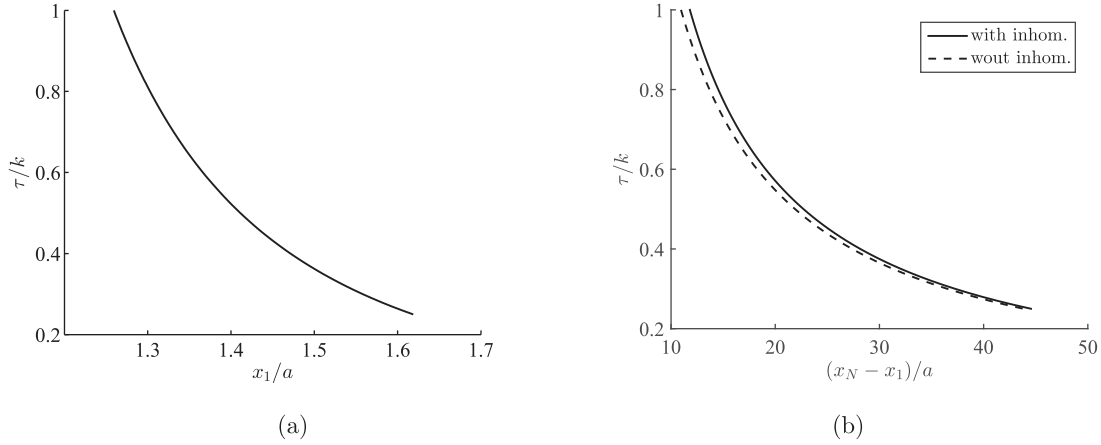

Fig. 4. (a) The position of the leading dislocation $\xi_1 = x_1/a$ in the pileup against a rigid inhomogeneity vs. the normalized applied shear stress τ/k in the case $N = 5$ and $\nu_1 = 1/3$. (b) The corresponding extent of the pileup $(\xi_N - \xi_1) = (x_N - x_1)/a$ vs. the applied shear stress τ/k.

However, from the equilibrium conditions of dislocations (11), we have

$$\sum_{j=1}^{N} f_{i,j}^{\text{image}} = -\left(f_i^{\text{appl}} + \sum_{j\neq i}^{N} f_{i,j}^{\infty} \right). \tag{14}$$

Consequently, by substituting (14) into (13), the total force on the inhomogeneity is

$$f_0 = -\sum_{i=1}^{N} f_i^{\text{appl}}, \tag{15}$$

because, by the action and reaction,

$$\sum_{i=1}^{N}\sum_{j\neq i}^{N} f_{i,j}^{\infty} = 0. \tag{16}$$

Finally, the incorporation of (7) into (15) gives

$$f_0 = \tau b_x \left[N + A \sum_{i=1}^{N} \left(\frac{2}{\xi_i^2} - \frac{3}{\xi_i^4} \right) \right]. \tag{17}$$

This force can be interpreted as the potential energy release rate associated with the increase of the distance between the inhomogeneity and the pileup, keeping the positions of all dislocations in the pileup fixed relative to each other. As such, the expression for this force could also be derived by an evaluation of the J integral around the inhomogeneity, but details of this derivation are omitted here. The part of the force $f_0^* = N\tau b_x$ is the force required to keep the leading dislocation pinned in the pileup within an infinite medium without the inhomogeneity (Eshelby et al., 1951).

2.3. Shear stress concentration in front of the inhomogeneity

The normalized shear stress at the interface between the inhomogeneity and the surrounding medium, at the point $(a, 0)$ of the slip plane of the pileup, is

$$\hat{\sigma}_{xy}(a,0) = -(1+A)\hat{\tau} + NA - \sum_{i=1}^{N} \left(2 + \frac{A-B}{\xi_i} \right) \frac{1}{\xi_i - 1}, \quad \xi_i = \frac{x_i}{a}. \tag{18}$$

Fig. 6a shows the variation of this stress with the ratio G_2/G_1 in the case of $N = 5$ dislocations in the pileup under remote stress $\hat{\tau} = 0.25$, which is arbitrarily selected for illustrative purposes. Since $\hat{\tau} = \tau/k$, where $k = k_1(b_x/a)$ and $k_1 = G_1/[\pi(\kappa_1 + 1)]$, there are infinitely many combinations of the actual applied stress τ and the ratio a/b_x which give $\hat{\tau} = 0.25$. The Poisson ratios are taken to be $\nu_1 = \nu_2 = 1/3$. The stiffer the inhomogeneity, the lower the magnitude of the stress $\sigma_{xy}(a, 0)$, because dislocations are more strongly repelled by stiffer inhomogeneity and find their equilibrium positions further away from the inhomogeneity. Fig. 6b shows a

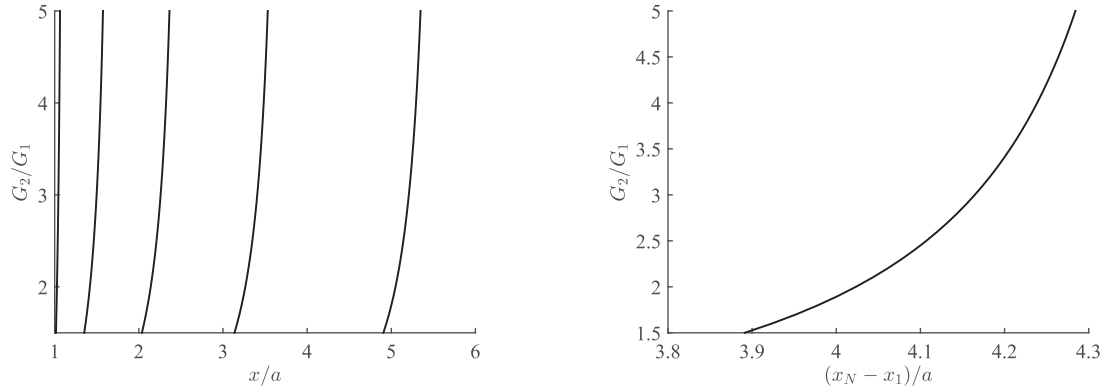

Fig. 5. (a) The equilibrium positions of $N = 5$ dislocations in a pileup against a circular inhomogeneity of radius a vs. the stiffness G_2/G_1. The applied shear stress is $\tau = 3k$, and it is assumed that $\nu_1 = \nu_2 = 1/3$. (b) The corresponding extent of the pileup.

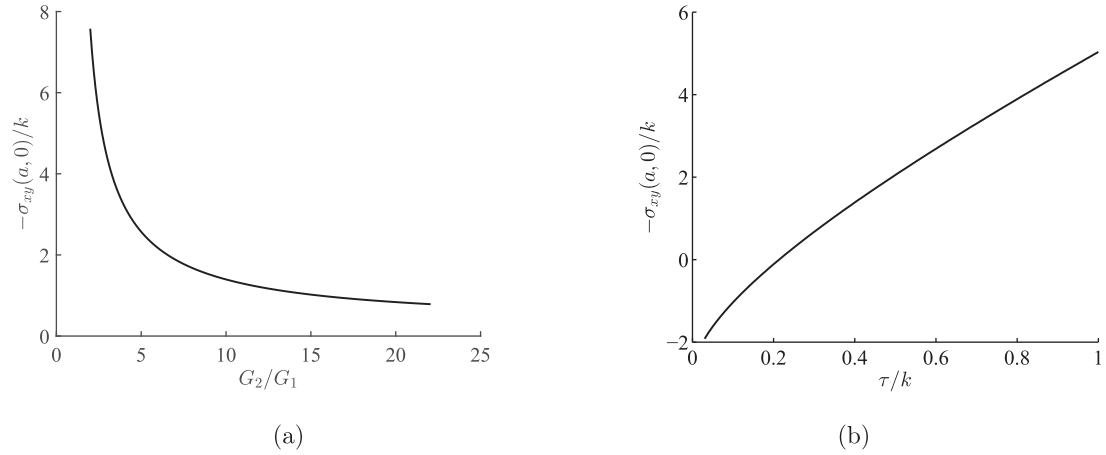

Fig. 6. (a) The variation of the stress $-\hat{\sigma}_{xy}(a,0) = -\sigma_{xy}(a,0)/k$ with the ratio G_2/G_1 in the case of $N = 5$ dislocations in the pileup under remote stress $\hat{\tau} = \tau/k = 0.25$. The Poisson ratios are taken to be $\nu_1 = \nu_2 = 1/3$. (b) The variation of $-\hat{\sigma}_{xy}(a,0)$ with the applied stress $\hat{\tau} = \tau/k$ in the case of 5 dislocations in a pileup against a rigid inhomogeneity. The Poisson ratio $\nu_1 = 1/3$.

nonlinear variation of $\sigma_{xy}(a, 0)$ with the applied stress τ in the case of $N = 5$ dislocations in a pileup against a rigid inhomogeneity.

For a fixed value of remote stress τ, large values of the nondimensional stress $\hat{\tau}$ correspond to large-size inhomogeneities (small ratio b_x/a), while for a fixed-size inhomogeneity, large values of $\hat{\tau}$ correspond to large values of the applied remote stress τ. Fig. 7 shows the variation of the normalized stress $-\sigma_{xy}(a,0)/k_1$ with the ratio a/b_x under the applied shear stress $\tau = 0.01k_1$. For large values of a/b_x the stress approaches the value corresponding to a pileup against a flat bimetallic interface, considered in Section 3. In case $\Gamma = 2$ (Fig. 7a) the maximum magnitude of the shear stress is $|\sigma_{xy}(a,0)|_{\max} = 0.316k_1$ (at $a = 7.4b_x$). This maximum stress scales linearly with τ.

Fig. 8 illustrates the effect of Poisson's ratio on $\sigma_{xy}(a, 0)$. Since different values of ν_1 lead to different values of k_1, the stress normalization is made with respect to the parameter $k_* = \mu_1 b_x/a$. The results for pileups with any other number of dislocations, or for any other combinations of material parameters, can be obtained and analyzed similarly.

3. Edge dislocation pileup against a flat bimetallic interface

Fig. 9 shows an edge dislocation pileup along the positive x axis orthogonal to a perfectly bonded bimetallic interface ($y = 0$). The shear stress along the positive x-axis produced by an edge dislocation at a distance $x = x_i$ from this interface can be obtained from the results presented in Section 2 for a dislocation against a circular inhomogeneity shown in Fig. 1a by performing the limiting process $a \to \infty$. Toward that, we rewrite (1) as

$$\bar{\sigma}_{xy}^{\text{disl}}(u,0) = \frac{2}{u-u_i} + (A+B)\frac{\bar{a}+u_i}{\bar{a}(u+u_i)+uu_i} + 2A\frac{\bar{a}^2 u_i(u-u_i)(2\bar{a}+u_i)}{[\bar{a}(u+u_i)+uu_i]^3} - (A+B)\frac{1}{\bar{a}+u} + (A-B)\frac{\bar{a}^2}{(\bar{a}+u)^2(\bar{a}+u_i)} + 2A\frac{\bar{a}^2}{(\bar{a}+u)^3}, \tag{19}$$

where the lengths are normalized by b_x, so that u is a normalized distance along the slip plane $y = 0$, measured from the boundary of the inhomogeneity ($x = a$) in Fig. 1a, i.e.,

$$u = \frac{x-a}{b_x}, \quad u_i = \frac{x_i - a}{b_x}, \quad \bar{a} = \frac{a}{b_x}, \quad \bar{\sigma}_{xy} = \frac{\sigma_{xy}}{k_1}, \quad k_1 = \frac{G_1}{\pi(\kappa_1+1)}. \tag{20}$$

The utilized material parameters A and B are defined by (3), in which (G_1, ν_1) and (G_2, ν_2) stand for the elastic properties of ma-

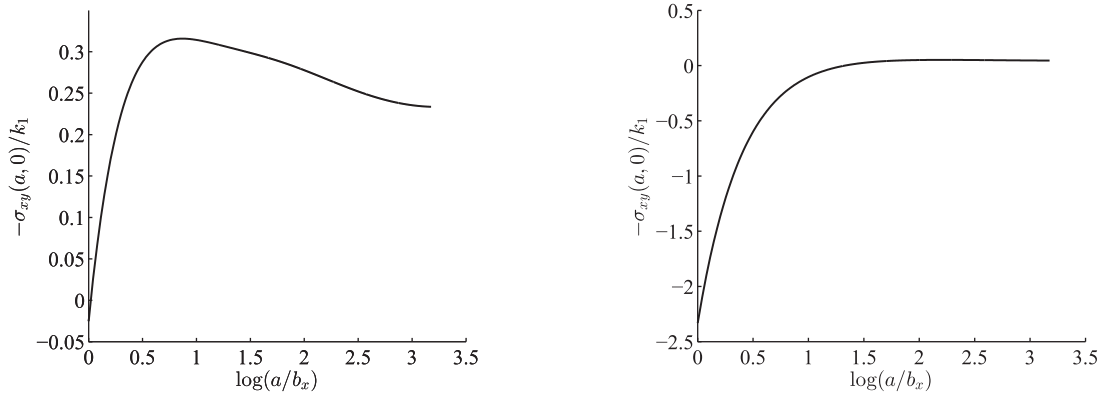

Fig. 7. (a) The variation of the normalized stress $-\sigma_{xy}(a,0)/k_1$ with the ratio a/b_x in the case of $N=5$ dislocations in the pileup under remote stress $\tau = 0.01k_1$. Part (a) is for $G_2/G_1 = 2$ and $\nu_1 = \nu_2 = 1/3$, while part (b) is for rigid inhomogeneity and $\nu_1 = 1/3$.

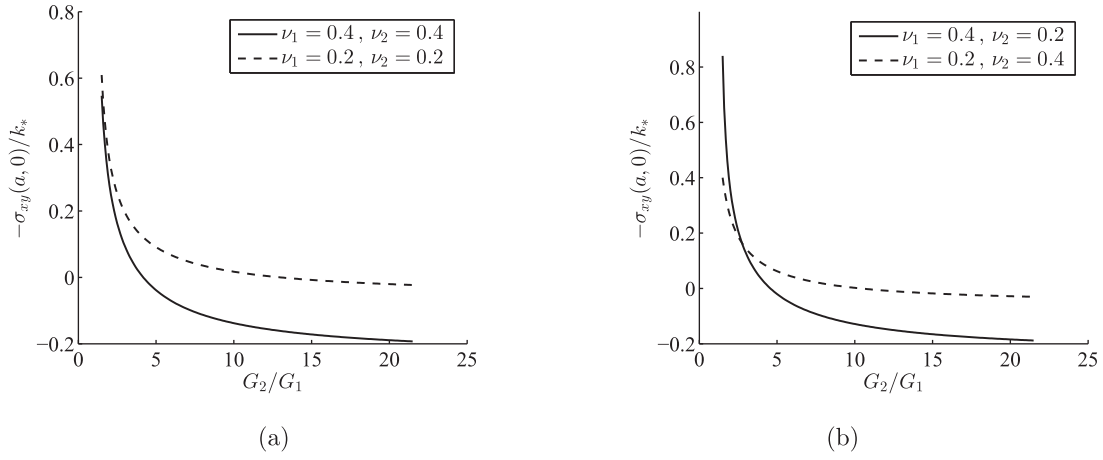

Fig. 8. The variation of the normalized stress $-\sigma_{xy}(a,0)/k_*$ with G_2/G_1 in the case of $N=5$ dislocations in the pileup under remote stress $\tau = 0.01k_*$, where $k_* = \mu_1 b_x/a$. The Poisson ratios are taken as indicated in the legends of parts (a) and (b).

terials (1) and (2). By performing the limit $\bar{a} \to \infty$, (19) reduces to

$$\bar{\sigma}_{xy}^{\rm disl}(\bar{x},0) = \frac{2}{\bar{x}-\bar{x}_i} + (A+B)\,\frac{1}{\bar{x}+\bar{x}_i} + 4A\,\frac{\bar{x}_i(\bar{x}-\bar{x}_i)}{(\bar{x}+\bar{x}_i)^3}\,, \quad \bar{x} = \frac{x}{b_x}\,, \tag{21}$$

which is the shear stress produced by an edge dislocation at a distance x_i from the bimetallic interface shown in Fig. 9. Expression (21) is equivalent to that of Dundurs (1969), who cast it in terms of the parameters

$$\alpha = \frac{(\kappa_1+1)\Gamma - (\kappa_2+1)}{(\kappa_1+1)\Gamma + (\kappa_2+1)}\,, \quad \beta = \frac{(\kappa_1-1)\Gamma - (\kappa_2-1)}{(\kappa_1+1)\Gamma + (\kappa_2+1)}\,. \tag{22}$$

The relationships among the two sets of parameters are

$$A+B = 2\,\frac{\alpha+\beta^2}{1-\beta^2}\,, \quad A = \frac{\alpha-\beta}{1+\beta}\,, \quad B = \frac{\alpha+\beta}{1-\beta}\,. \tag{23}$$

In particular, Dundurs (1969) has shown that a dislocation is repelled by the interface if $\alpha - \beta^2 > 0$ or ($\alpha - \beta^2 < 0$, $\alpha + \beta^2 > 0$).

The nonsingular portion of the shear stress (21) at the position of the dislocation is

$$\bar{\sigma}_{xy}^{\rm disl}(\bar{x}_i,0) = (A+B)\,\frac{1}{2\bar{x}_i}\,. \tag{24}$$

The configurational force exerted by the interface on the dislocation at $x = x_i$ is the image force from that dislocation, $f_{i,i}^{\rm image} = \sigma_{xy}^{\rm disl}(x_i,0)b_x$. In view of (24), this is, in a dimensionless form,

$$\bar{f}_{i,i}^{\rm image} = (A+B)\,\frac{1}{2\bar{x}_i}\,, \quad \bar{f} = \frac{f}{k_1 b_x} \tag{25}$$

If a bimetallic material is subjected to a uniform remote stress $\sigma_{xy}^{\infty} = -\tau$, the shear stress σ_{xy} along the x-axis (and everywhere in the material) is equal to $-\tau$. Thus, the configurational force exerted on the dislocation by the externally applied remote stress is $f_i^{\rm appl} = -\tau b_x$, or, when normalized,

$$\bar{f}_i^{\rm appl} = -\bar{\tau}\,, \quad \bar{\tau} = \frac{\tau}{k_1}\,. \tag{26}$$

If there are two alike edge dislocations in the material (1), one at a distance $x = x_i$ and the other at a distance $x = x_j$ from the interface, there is an additional contribution to the force on the dislocation at $x = x_i$ due to its interaction with the dislocation at $x = x_j$. This is $f_{i,j} = f_{i,j}^{\infty} + f_{i,j}^{\rm image}$, where, upon normalization,

$$\bar{f}_{i,j}^{\infty} = \frac{2}{\bar{x}_i - \bar{x}_j}\,, \quad \bar{f}_{i,j}^{\rm image} = (A+B)\,\frac{1}{\bar{x}_i+\bar{x}_j} + 4A\,\frac{\bar{x}_j(\bar{x}_i-\bar{x}_j)}{(\bar{x}_i+\bar{x}_j)^3}\,. \tag{27}$$

If there are N dislocations in a pileup of edge dislocations (Fig. 9), the total force on a dislocation at x_i is specified by expression (10), so that the equilibrium positions of dislocations are

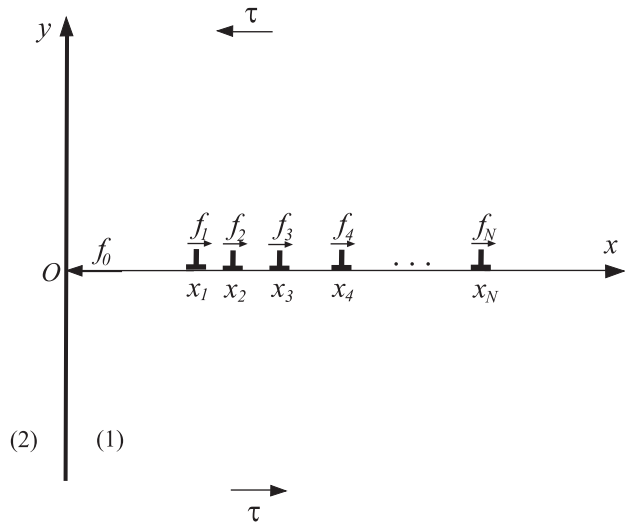

Fig. 9. A pileup of N edge dislocations against a bimetallic interface between the materials (1) and (2) under applied remote uniform shear stress τ. The configurational force exerted on the interface by the pileup is f_0. In the equilibrium configuration the configurational force on each dislocation vanishes ($f_i = 0$).

obtained by solving a system of equations

$$\sum_{j=1}^{N}\left[(A+B)\,\frac{1}{\bar{x}_i+\bar{x}_j}+4A\,\frac{\bar{x}_j(\bar{x}_i-\bar{x}_j)}{(\bar{x}_i+\bar{x}_j)^3}\right] + \sum_{j\neq i}^{N}\frac{2}{\bar{x}_i-\bar{x}_j}=\bar{\tau}\,, \quad (i=1,2,3,\ldots N). \tag{28}$$

If the shear stress is changed from, say, τ_0 to $c\tau_0$ ($c>0$), from (28) it follows that the corresponding equilibrium positions of dislocations change from x_i^0 to x_i^0/c. The extent (length) of the pileup changes from $L^0 = x_N^0 - x_1^0$ to L_0/c. Also, by an analogous analysis to that used in Section 2.3, the configurational force on the interface from the dislocation pileup is

$$f_0 = -\sum_{i=1}^{N} f_i^{\text{appl}} = N\tau b_x\,. \tag{29}$$

Fig. 10a shows the equilibrium positions of $N = 5$ dislocations in a pileup under remote stress $\tau = 0.1k_1$ against a bimetallic interface corresponding to different values of $\Gamma = G_2/G_1$ and the same values of the Poisson ratio $\nu_1 = \nu_2 = 1/3$. The pileup is further away from the interface for greater values of Γ, due to the correspondingly stronger repulsion of the interface. Fig. 10b shows the extent of the pileup, which increases with the increase of Γ. The dashed-line is the (constant) extent of the pileup in a homogeneous medium with the pinned leading dislocation, obtained from the Eshelby et al. (1951) solution, which is independent of Γ.

Fig. 11 shows the evolution of the equilibrium pileup configurations under the increasing remote shear stress τ (scaled by k_1). Fig. 11a is for the pileup against a rigid interface, and Fig. 11b for the pileup against an interface with $\Gamma = 2$ and $\nu_1 = \nu_2 = 1/3$. The results corresponding to other values of Γ and (ν_1, ν_2) can be obtained similarly.

3.1. Stress concentration along the interface

The pileup dislocations cause large tensile stresses at the interface below the slip plane of positive edge dislocations, as well as large shear stress at the intersection of the interface with the slip plane of dislocations. Since these stresses may cause interface cracking, it is of interest to evaluate them. The normal and shear stresses (σ_x, σ_{xy}) along the interface can be obtained by superposition of contributions from individual dislocations. From the stress expressions listed by Lubarda (1997) and Asaro and Lubarda (2006), we obtain

$$\bar{\sigma}_x(0,\bar{y}) = -2c_1\bar{y}\sum_{i=1}^{N}\frac{1}{\bar{x}_i^2+\bar{y}^2}\left(c_2+\frac{3\bar{x}_i^2+\bar{y}^2}{\bar{x}_i^2+\bar{y}^2}\right), \tag{30}$$

$$\bar{\sigma}_{xy}(0,\bar{y}) = -\bar{\tau}+2c_1\sum_{i=1}^{N}\frac{\bar{x}_i}{\bar{x}_i^2+\bar{y}^2}\left(c_2-\frac{\bar{x}_i^2-\bar{y}^2}{\bar{x}_i^2+\bar{y}^2}\right), \tag{31}$$

where $\bar{x}_i = x_i/b_x$, $\bar{y} = y/b_x$, and

$$c_1 = \frac{1+\alpha}{1+\beta}\,, \quad c_2 = \frac{\beta}{1-\beta}\,. \tag{32}$$

Expressions (30) and (31) are equivalent to expressions (11)–(13) of Öveçoğlu et al. (1987), expressed in dimensionless form by using the length parameter $D = 2k_1 b_x/\tau$, though they were left in a slightly less compact form than expressions (30)–(32) here. At the intersection of the interface and the slip plane of dislocations, the shear stress is

$$\bar{\sigma}_{xy}(0,0) = -\bar{\tau}-2c_1(1-c_2)\sum_{i=1}^{N}\frac{1}{\bar{x}_i}\,, \tag{33}$$

which is the largest shear stress σ_{xy} along the interface. In view of the discussion following (28), it also follows that $\sigma_{xy}(0,0)$ depends linearly on τ. We also note that both $\sigma_x^\tau(0,y)$ and $\sigma_{xy}^\tau(0,y)$ obey

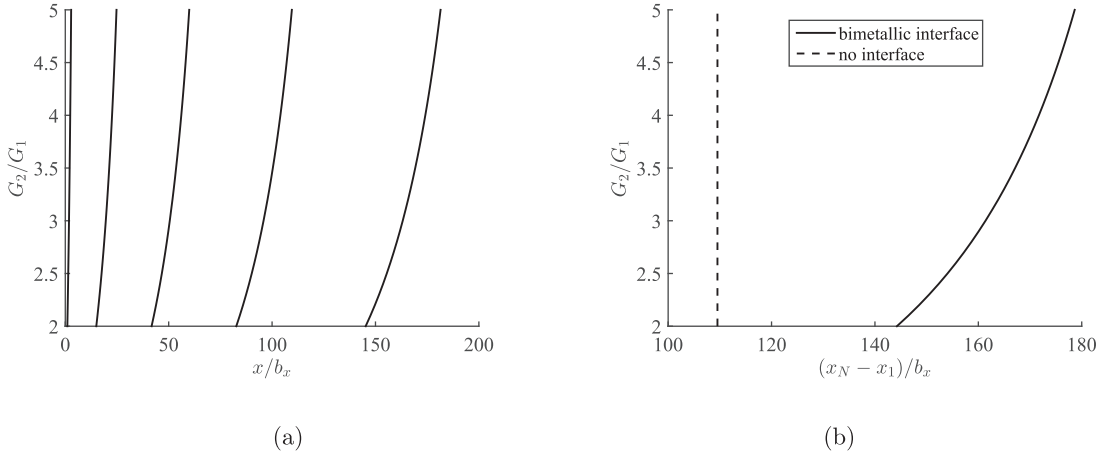

Fig. 10. (a) The equilibrium positions of $N = 5$ edge dislocations in a pileup under shear stress $\tau = 0.1k_1$ against a bimetallic interface with different values of $\Gamma = G_2/G_1$ and the same value of the Poisson ratio $\nu_1 = \nu_2 = 1/3$. (b) The corresponding extent of the pileup.

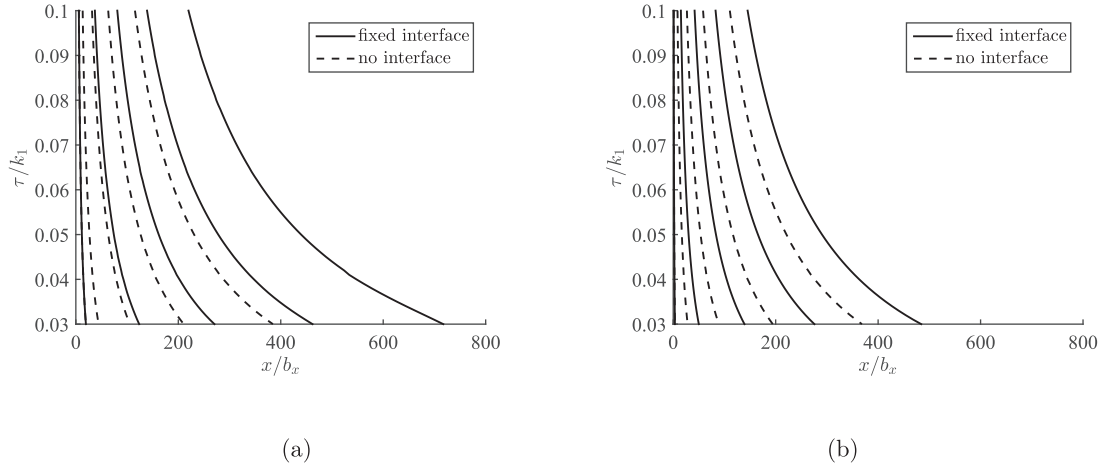

Fig. 11. (a) The equilibrium positions of $N = 5$ edge dislocations vs. the applied shear stress $\bar{\tau} = \tau/k_1$ in a pileup against a rigid interface ($\Gamma = \infty$, $\nu_1 = 1/3$). (b) The same as in (a), for a bimetallic interface with $\Gamma = 2$ and $\nu_1 = \nu_2 = 1/3$.

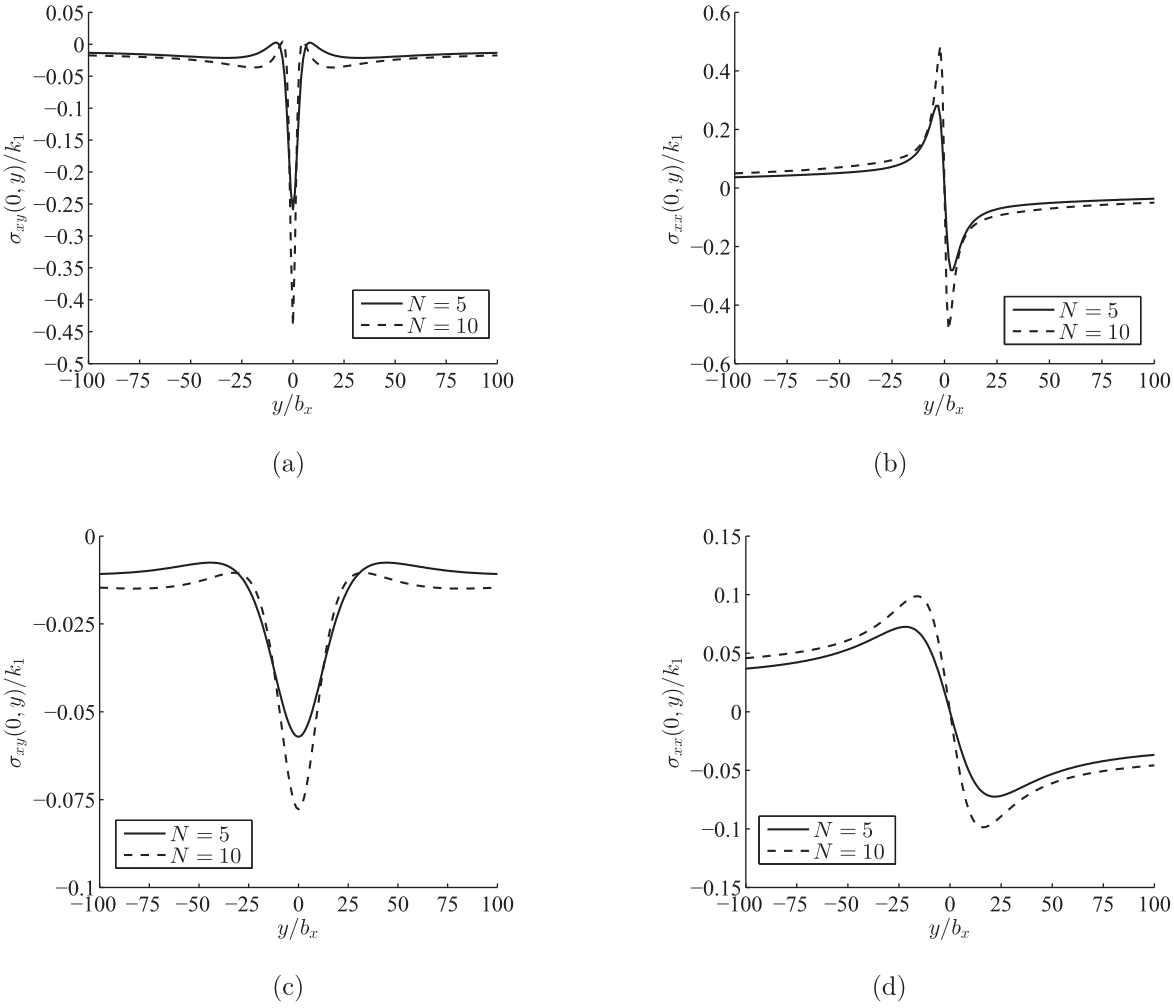

Fig. 12. (a) Shear stress σ_{xy} along the y axis for pileups of 5 and 10 dislocations in the case $\Gamma = 2$ and $\nu_1 = \nu_2 = 1/3$. The applied stress is $\tau = 0.01k_1$. (b) The corresponding variation of the normal stress σ_{xx}. (c) & (d) Same as (a) & (b), in the case $\Gamma = \infty$.

the following property with respect to the change of the applied stress from τ to $c\tau$ ($c > 0$),

$$\sigma_x^{c\tau}(0, y/c) = c\sigma_x^{\tau}(0, y)\,, \quad \sigma_{xy}^{c\tau}(0, y/c) = c\sigma_{xy}^{\tau}(0, y)\,, \tag{34}$$

which follows by dimensional considerations. Thus, if σ_x^{τ} has its maximum along the interface at $y = y_*$, $\sigma_x^{c\tau}$ has its maximum at $y = y_*/c$, and $(\sigma_x^{c\tau})_{\max} = c(\sigma_x^{\tau})_{\max}$. Similar property holds for the shear stress σ_{xy} along the interface, except that in this case the maximum always occurs at $y = 0$.

Figs. 12a and b show the stresses along the interface in the case of $N = 5$ and 10 dislocations piled-up against the interface with $\Gamma = 2$ and $\nu_1 = \nu_2 = 1/3$, under the remote stress $\tau = 0.01k_1$.

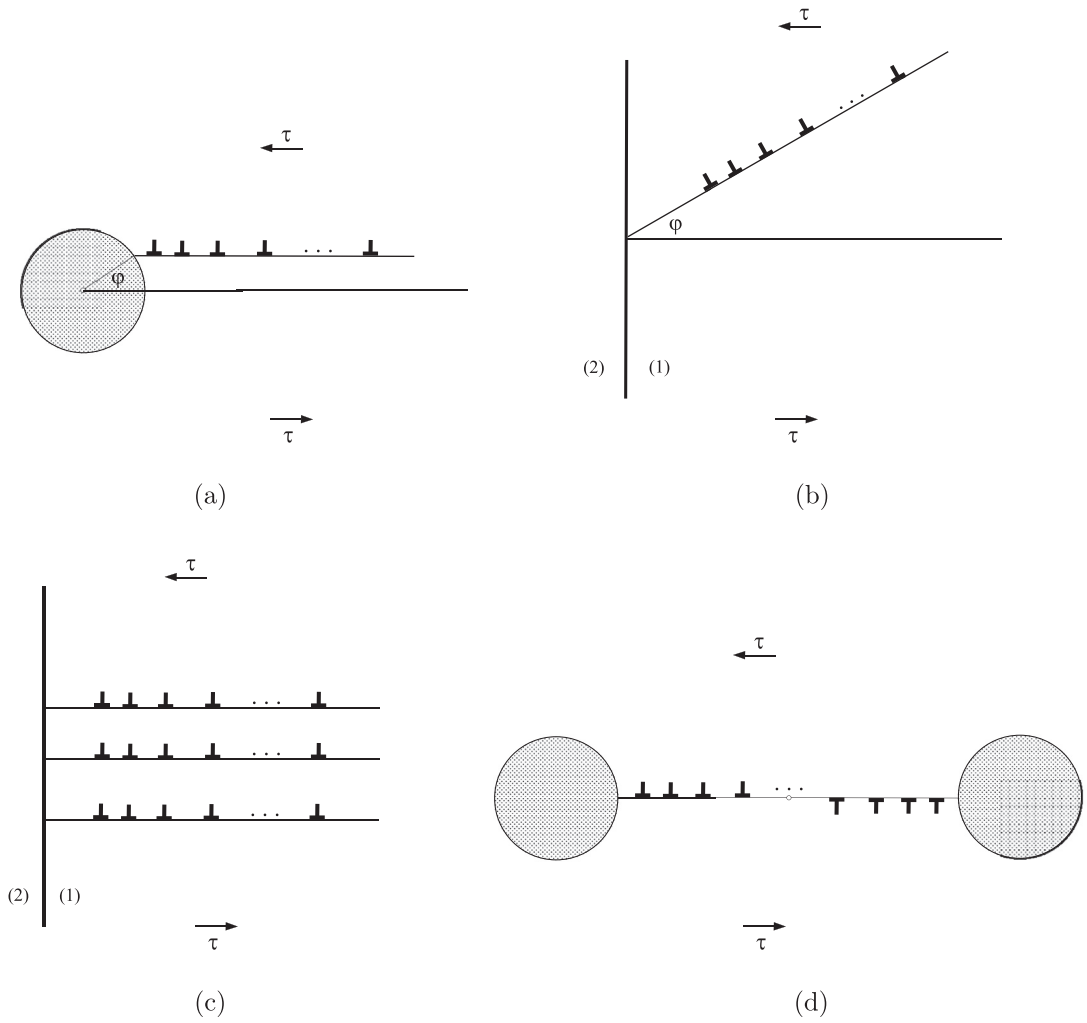

Fig. 13. (a) A dislocation pileup against a circular inhomogeneity along an eccentric slip plane at an angle φ relative to the horizontal centroidal axis. (b) A dislocation pileup against a plane bimetallic interface along a slip plane at an angle φ relative to the horizontal axis. (c) Several pileups on parallel slip planes against a plane bimetallic interface. (d) A stressed double pileup between two inhomogeneities under remote shear stress τ.

The stress concentration is decreased in the case of pileups against a harder interface (larger Γ), because dislocation equilibrium positions are further away from such interface. This is illustrated in Fig. 12c and d. Poisson ratios may also considerably affect the interface stresses, which has been examined by Kuan and Hirth (1976), and Öveçoğlu et al. (1987). The observed trend is that the increase of ν_1 increases the maximum interface stress, while the increase of ν_2 decreases the stress, both being associated with the effect of ν_1/ν_2 on the intensity of the repulsion exerted by the interface on the dislocations and the proximity of the leading dislocation to the interface.

It is noted that a pileup can form even in the absence of shear modulus disparity ($\Gamma = 1$), due to the Poisson ratio disparity, provided that $\nu_2 > \nu_1$. In this case, $A = 0$ and the system of equations (28) reduces to

$$\sum_{j=1}^{N} \frac{B}{\bar{x}_i + \bar{x}_j} + \sum_{j\neq i}^{N} \frac{2}{\bar{x}_i - \bar{x}_j} = \bar{\tau}\,, \quad (i = 1, 2, 3, \ldots N)\,, \tag{35}$$

where

$$B = \frac{2\alpha}{1-\alpha} = \frac{\nu_2 - \nu_1}{1 - \nu_2}\,, \quad \alpha = \beta = \frac{\nu_2 - \nu_1}{2 - (\nu_1 + \nu_2)}\,. \tag{36}$$

The system of Eqs. (35) has the solution provided that $B > 0$, i.e., $\nu_2 > \nu_1$. For example, if only one dislocation is near the interface, the shear stress required to hold it in equilibrium at a distance x_1 from the interface is $\bar{\tau} = B/(2\bar{x}_1)$, i.e.,

$$\tau = \frac{G_1}{8\pi} \frac{\nu_2 - \nu_1}{(1-\nu_1)(1-\nu_2)} \frac{b_x}{x_1}\,. \tag{37}$$

For τ to be positive, B must be positive, i.e., $\nu_2 > \nu_1$.

4. Conclusions

The pileups of discrete edge dislocations against a circular inhomogeneity within an infinite isotropic matrix, or against a flat bimetallic interface were considered. The equilibrium configurations of pileups under remote shear loading were determined by solving numerically the nonlinear algebraic equations representing the equilibrium conditions of the vanishing Peach–Koehler force for each of N dislocations in a pileup. The increase of the applied stress moves a pileup closer to the inhomogeneity and increases the density of dislocations within a pileup. This is more pronounced for smaller and softer inhomogeneities, due to their weaker repulsion of dislocations. The configurational force exerted on the inhomogeneity by a pileup is the sum of the local Peach–Koehler forces from the remote loading only, and is thus equal to $N\tau b_x$ plus a term dependent on dislocation positions and material properties. The stiffer the inhomogeneity, the smaller the configu-

rational force, for any given level of applied shear stress. The magnitude of the shear stress at the interface between the inhomogeneity and the matrix along the slip plane of dislocations is evaluated. This stress decreases with the increase of the ratio $G_2/G_1 > 1$ between the shear stiffness of the inhomogeneity and the surrounding matrix material. The configurational force exerted on a plane bimetallic interface by a pileup of N dislocations is equal to $N\tau b_x$, independently of dislocation positions and material properties. The shear and normal stress concentration is evaluated along the interface. The maximum shear and normal stresses at the interface change linearly with τ. If σ_x^τ due to shear stress τ has its maximum along the interface at $y = y_*$, $\sigma_x^{c\tau}$ has its maximum at $y = y_*/c$ and $(\sigma_x^{c\tau})_{\max} = c(\sigma_x^\tau)_{\max}$. Similar property holds for the shear stress σ_{xy} along the interface. The stress concentration at the interface depends strongly on both the shear moduli and the Poisson ratios of two materials. The general trend is that the increase of the shear modulus and Poisson's ratio disparities (G_2/G_1 and ν_2/ν_1) diminishes the interface stresses due to the stronger repulsion exerted by the interface on the piled-up dislocations, whose equilibrium positions are in that case more distant from the interface.

A worthwhile extension of the present work is the consideration of the pileup configurations shown in Fig. 13. Part (a) shows a dislocation pileup against a circular inhomogeneity along an eccentric slip plane, while part (b) shows a dislocation pileup against a bimetallic interface along a slip plane at an angle φ relative to the horizontal axis. Fig. 13c shows several pileups on parallel slip planes against a plane bimetallic interface. More difficult is the analysis of stressed double pileups between two inhomogeneities (Fig. 13d) because of the absence of an analytical solution for the edge dislocation between two inhomogeneities, although large radius inhomogeneities which are far enough apart could possibly be handled by a perturbation analysis, as pointed out to me by one of the reviewers. These studies, as well as the incorporation of the effects of the boundary of a finite body in which the pileups reside, can be done numerically by using the finite element method and the methodology developed by Lubarda et al. (1993) in their study of equilibrium dislocation distributions.

Acknowledgments

Research support from the Montenegrin Academy of Sciences and Arts and discussions with Professor David M. Barnett from Stanford University are gratefully acknowledged. I also thank anonymous reviewers for their helpful comments and suggestions.

References

Asaro, R.J., Lubarda, V.A., 2006. Mechanics of Solids and Materials. Cambridge Univ. Press, Cambridge.
Barnett, D.M., 1967. The effect of shear modulus on the stress distribution produced by a planar array of screw dislocations near a bi-metallic interface. Acta metall. 15, 589–594.
Barnett, D.M., Tetelman, A.S., 1966. The stress distribution produced by screw dislocation pile-ups at rigid circular cylindrical inclusions. J. Mech. Phys. Solids 14, 329–348.
Barnett, D.M., Tetelman, A.S., 1967. The stresses produced by a screw dislocation pileup at a circular inclusion of finite rigidity. Can. J. Phys. 45, 841–863.
Chou, Y.T., 1965. Linear dislocation arrays in heterogeneous materials. Acta metall. 13, 779–783.
Chou, Y.T., 1966. Equilibrium of linear dislocation arrays in heterogeneous materials. J. Appl. Phys. 37, 2425–2429.
Coleman, T.F., Li, Y., 1994. On the convergence of interior-reflective Newton methods for nonlinear minimization subject to bounds. Math. Program. 67, 189–224.
Conn, A.R., Gould, N.I.M., Toint, P.L., 2000. Trust Region Methods. MOS-SIAM series on optimization. Society for Industrial and Applied Mathematics.
Dundurs, H., Mura, T., 1964. Interaction between an edge dislocation and a circular inclusion. J. Mech. Phys. Solids 12, 177–189.
Dundurs, J., 1969. Elastic interactions of dislocations with inhomogeneities. In: Mura, T. (Ed.), Mathematical Theory of Dislocations. ASME, New York, pp. 70–115.
Eshelby, J.D., Frank, F.C., Nabarro, F.R.N., 1951. The equilibrium of linear arrays of dislocations. Phil. Mag. 42, 351–364.
Hall, C.L., 2010. Asymptotic expressions for the nearest and furthest dislocations in a pile-up against a grain boundary. Phil. Mag. 90, 3879–3890.
Hirth, J.P., Lothe, J., 1982. Theory of Dislocations. John Wiley & Sons, New York.
Kuan, H., Hirth, J.P., 1976. Dislocation pileups near the interface of a bimaterial couple. Mater. Sci. Eng. 22, 113–131.
Kuang, J.G., Mura, T., 1968. Dislocation pile-up in two-phase materials. J. Appl. Phys. 39, 109–120.
Lubarda, V.A., 1997. Energy analysis of edge dislocation arrays near bimaterial interfaces. Int. J. Solids Struct. 34, 1053–1073.
Lubarda, V.A., Blume, J.A., Needleman, A., 1993. An analysis of equilibrium dislocation distributions. Acta Metall. Mater. 41, 625–642.
Lubarda, V.A., Markenscoff, X., 1999. Energies of circular inclusions with sliding and bonded interfaces. Proc. Roy. Soc. Lond. A 455, 961–974.
Öveçoğlu, M.L., Barnett, D.M., Nix, W.D., 1987. Analysis of the interfacial stresses produced by a pile-up of discrete edge dislocations in two phase materials. Acta metall. 35, 1779–1789.
Smith, E., 1972. The stress distribution near the tip of an array of screw dislocations piled-up against an inclusion. J. Mech. Phys. Solids 20, 307–312.
Thölén, A.R., 1970. The stress field of a pile-up of screw dislocations at a cylindrical inclusion. Acta metall. 18, 445–455.
Voskoboinikov, R.E., Chapman, S.J., McLeod, J., Ockendon, J.R., 2009. Asymptotics of edge dislocation pile-up against a bimetallic interface. Math. Mech. Solids 14, 284–295.
Voskoboinikov, R.E., Chapman, S.J., Ockendon, J.R., 2007. Continuum and discrete models of dislocation pile-ups. II. Pile-up of screw dislocations at the interface in a bimetallic solid. Phil Mag. Lett. 87, 669–676.
Wagoner, R.H., 1981. Calculating dislocation spacings in pile-ups at grain boundaries. Metall. Trans. A 12A, 2015–2023.